AIAA JOURNAL
Vol. 38, No. 8, August 2000

Analysis of Random Gust Response with Nonlinear Unsteady Aerodynamics

Yan-Nian Lee* and C. Edward Lan†
University of Kansas, Lawrence, Kansas 66045

Experimental nonlinear unsteady aerodynamics is employed to determine the maximal aircraft response to random gust through matched filter theory. Two airplane configurations, the F-18 High Alpha Research Vehicle (HARV) and F-16XL, have been tested in forced oscillation to provide the necessary data. The atmospheric turbulence is assumed to be characterized by the von Kármán gust power spectral density function. The nonlinear aerodynamic models are set up through Fourier functional analysis of the test data. For comparative purposes, linear aerodynamic models are also calculated by using the unsteady quasi-vortex-lattice method. It is shown that nonlinear unsteady aerodynamics produce the instantaneous maximum lift response to gust significantly higher than that by the linear unsteady aerodynamics. In plunging motion, the calculated results show that the use of nonlinear unsteady aerodynamics again results in much higher maximum gust load factors than with linear unsteady aerodynamics.

Nomenclature

C_L = lift coefficient
C_{L_g} = lift coefficient due to random gust
C_{L_m} = lift coefficient due to airplane's motion
C_{L_α} = variation of lift coefficient with angle of attack
$\bar{c}$ = mean aerodynamic chord
G = approximate von Kármán turbulence transfer function
g = gravitational acceleration
H_y = transfer function of combined airplane dynamics and gust
h_y = impulsive response
I = imaginary part of a complex number
K = constant
k = reduced frequency, $\omega\bar{c}/V$
L = scale of turbulence
L_g = lift due to random gust
L_m = lift due to airplane's motion
M = mass of airplane
S = wing surface area
s = Laplace transform variable
t_0 = time delay
t' = nondimensional time, $Vt/\bar{c}$
V = freestream velocity
W_g = vertical gust velocity/V
X = excitation waveform in the frequency domain
x = excitation waveform
Y = airplane response in the frequency domain
y = airplane response
z = vertical displacement, positive downward
α = angle of attack
$\dot{\alpha}$ = time rate of change of angle of attack
Δn = incremental load factor
$\delta(t)$ = impulse function
σ_y = root mean square of response y
τ = time variable or time interval
$\Phi_{W_g W_g}$ = power spectral density function of turbulence
ω = circular frequency

Introduction

GUSTS in nature tend to be random. They affect many aspects of airplane flight operations including control, dynamic structural loads, and flight safety. An airplane is designed to have sufficient strength in its structure to withstand loads from landing, maneuvering, random gust, etc. In the present investigation, only gust response will be considered. In analysis, a random gust is frequently represented by a statistical model, and the lift response of wings is assumed to be proportional to the gust velocity.[1] The early design methods for gust loads were based on a single discrete gust. The loads were determined by assuming a one-minus-cosine gust velocity profile confining the airplane motion to plunging only. Most works performed prior to the 1950s were based on these simplifications. More recently, the statistical discrete gust (SDG) method was developed. The SDG method is still being used in Great Britain in the verification of airplane gust response. In the United States, the power spectral density (PSD) method is used to define gust design loads that are specified in U.S. Federal Aviation Regulations (FAR) 25 (Ref. 2).

In the estimation of gust loads on airplanes, the maximum response to random gust is of main interest, especially for the structural design purpose. Perry et al.,[3] applied both the SDG method and the PSD method to an airplane with linear aerodynamics to calculate the maximum gust loads. Because of the exhaustive search algorithm of the SDG method, the computational cost was significantly larger than that of the PSD analysis.[3] However, the PSD method was only applied to a linear system. Scott et al. used a scheme based on matched filter theory (MFT) on linear[4] and nonlinear[5–7] airplane models to determine the maximum gust loads. The nonlinear model consisted of an airplane with linear aerodynamics and nonlinear controllers. The aerodynamics were calculated by using the doublet-lattice method (DLM), which is a linear aerodynamic theory. The von Kármán turbulence transfer function served as a filter for airplane response to turbulence.

In the present investigation, the system consists of a gust model described by von Kármán's PSD function and an airplane unsteady lift model that can be linear or nonlinear. The nonlinear unsteady aerodynamic models used here are developed from forced-oscillation test data and are approximately linear in the amplitude of angle-of-attack oscillation, but quite different in the magnitude of frequency-dependent response from the linear theory.

Theoretical Development

To assess the effect of nonlinear unsteady aerodynamics, two types of gust response will be investigated: 1) instantaneous maximum lift response without the airplane motion and 2) maximum load factor in vertical plunging. The MFT method will be used to obtain the maximum gust response. The MFT and the mathematical formulation for the maximum gust response is summarized in the following.

Received 30 November 1998; revision received 16 September 1999; accepted for publication 22 December 1999.

*Graduate Student, Department of Aerospace Engineering.
†J. L. Constant Distinguished Professor, Department of Aerospace Engineering. Associate Fellow AIAA.

MFT Method

In the MFT method, the excitation $x(t)$ that produces the maximum response $y(t)$ has the same waveform as the response waveform reversed in time and shifted by a time delay t_0 (see Ref. 8 for proof). The corresponding unit impulse response $h_y(t)$ of output y can be expressed as[4]

$$h_y = Kx(-t + t_0) \tag{1}$$

Therefore, the input excitation to produce the maximum response can be determined from the system's unit impulse response:

$$x(t) = h_y(t_0 - t)/K \tag{2}$$

where K is chosen to be the root mean squares of the impulsive response to normalize the energy of the excitation waveforms.[4] To demonstrate this, take Fourier transform of the impulsive response $h_y(t)$ and output $y(t)$ to give

$$H_y(\omega) = KX^*(\omega)\, e^{-i\omega t_0}, \qquad Y(\omega) = H_y(\omega)X(\omega) \tag{3}$$

where the superscript* means complex conjugate. From the definition of the mean square, the energy content of the impulsive response function $h_y(t)$ is

$$h_y^2(t) = \frac{K^2}{2\pi}\int_{-\infty}^{\infty} |X(\omega)|^2\, \mathrm{d}\omega = \sigma_y^2 \tag{4}$$

If $K = \sigma_y$, then

$$\frac{1}{2\pi}\int_{-\infty}^{\infty} X^*(\omega)X(\omega)\, \mathrm{d}\omega = 1 \tag{5}$$

The response of output $y(t)$ is, thus,

$$y(t) = \frac{K}{2\pi}\int_{-\infty}^{\infty} X^*(\omega)X(\omega)\, e^{i\omega(t - t_0)}\, \mathrm{d}\omega \tag{6}$$

At $t = t_0$, $y(t)$ is maximized and equals the root mean square of the impulsive response, that is,

$$y_{\max} = y(t_0) = \sigma_y \tag{7}$$

For a linear system, the application of this excitation waveform $x(t)$ will produce the time history of the output $y(t)$, within which the maximum response is a global maximum at a specific time t_0.

In the present investigation, the combined gust and linear (or nonlinear) airplane aerodynamics are referred to as a system with known dynamics. An impulse of infinite magnitude and infinitesimal duration does not occur in nature; however, if the pulse duration is much smaller than the time constant of the system, a representation of the input by an impulse is a good approximation. Therefore, imposing a unit impulse on the combined system, the output response provides the impulse response of the airplane:

$$h_y(t) = \int_0^{\infty} h_y(\tau)\delta(t - \tau)\, \mathrm{d}\tau \tag{8}$$

Physically, $h_y(\tau)\delta(t - \tau)$ is the impulse at time τ of magnitude $h_y(\tau)$ (Ref. 9). Applying a Fourier transform, the impulsive response in the frequency domain can be easily shown to be

$$\mathscr{F}[h_y(t)] = \bar{H}_y(\omega) \tag{9}$$

This relation is still valid with the nonlinear aerodynamics used here because the term nonlinear refers only to the relation between the unsteady lift coefficient and the angle of attack being different from the linear theory. The lift model is expressed in an indicial time integral that can be Fourier transformed. This will be explained further later.

With the knowledge of system's impulsive response being $h_y(t)$, the excitation $x(t)$ can be obtained from Eq. (2). The excitation is then the new input to the combined system. At a specified time t_0, the response is maximized. Therefore, the MFT method allows direct determination of the optimal input signal without using the calculus of variations.

Maximum Lift Response due to Random Gust

In the present study, the airplane response to random gust is based on nonlinear unsteady aerodynamic data and the MFT method. The detailed procedures can be explained by using a flow chart[7] shown in Fig. 1. Figure 1 shows the determination of the critical gust profile in the upper part and the corresponding maximum gust response in lift in the lower part. As shown in the upper part, the impulsive response $h_y(t)$ is first generated. An approximate von Kármán's gust

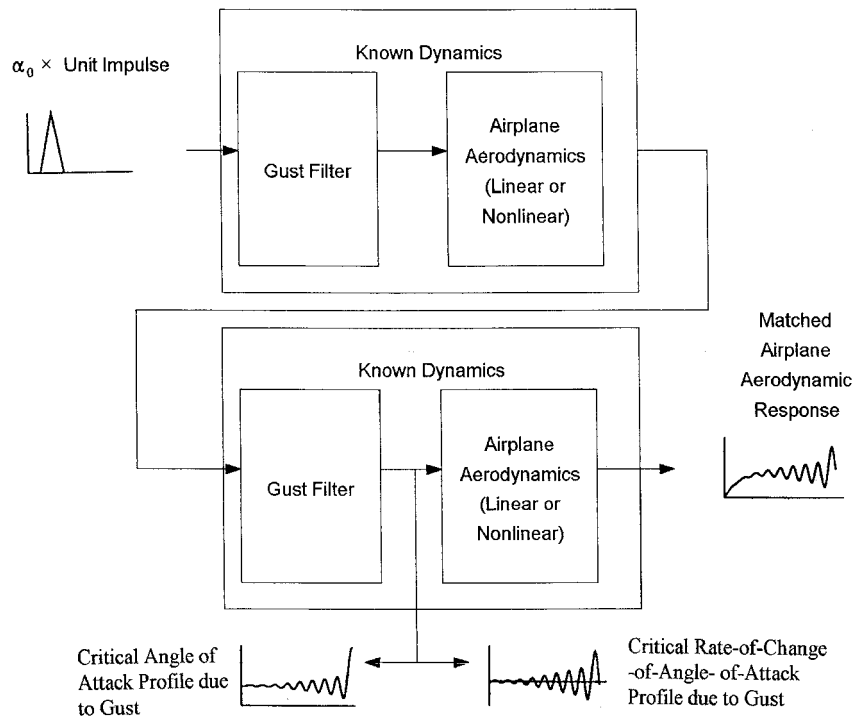

Fig. 1 Flowchart of the MFT method with linear or nonlinear aerodynamics.

filter $G(s)$ is used to generate the effect of atmospheric turbulence and is given as[10]

$$G(s) = \left(\frac{\sigma_g}{V}\right)\sqrt{\frac{L}{\pi V}} \times \frac{[1 + 2.618(L/V)s][1 + 0.1298(L/V)s]}{[1 + 2.083(L/V)s][1 + 0.823(L/V)s][1 + 0.0898(L/V)s]} \tag{10}$$

which approximates the square root of the von Kármán PSD function. The reason for using this approximate gust filter instead of the original von Kármán expression is that $G(s)$ is in the s domain and can be easily transformed into the frequency domain by substituting $i\omega$ for s. The gust filter is connected in series with nonlinear or linear aerodynamics, and together they serve as the known dynamics. With an impulse input to the gust filter, $\alpha_0\delta(t)$, whose Fourier transform equals α_0, a gust impulsive response is generated. Then, the output of the airplane aerodynamic model is the impulsive response of lift $h_y(t)$. In the conventional notation, $h_y(t)$ equals $C_L(t)$. In the frequency domain, the response can be written as

$$H_y(\omega) = \alpha_0 \bar{H}_y(\omega) G(\omega) \tag{11}$$

where $\bar{H}_y(\omega)$ is the lift impulsive response function and is given by the frequency response function in lift obtained through analysis of α oscillation test data.[11] According to Ref. 11, the harmonic response $\bar{H}_y(\omega)$ is calculated with the indicial–integral aerodynamic model that was established from large-amplitude forced oscillation. In the reduced frequency domain, the expression of the harmonic response $\bar{H}_y(\omega)$ is changed to $\bar{H}_y(k)$, which is given by

$$\begin{aligned}\bar{H}_y(k) &= H_{\text{av}}(k) + \sum_{j=1}^{m}\left(E_{1j}\dot{\alpha}_{b_j} + E_{2j}\ddot{\alpha}_{b_j}\right) \\ &\quad + C_1(H_{11}\alpha_b + H_{21}\dot{\alpha}_b)(1 - PD_1) \\ &\quad + C_2\left(H_{12}\alpha_b^2 + H_{22}\alpha_b\dot{\alpha}_b + H_{32}\dot{\alpha}_b^2\right)(1 - PD_2) + \cdots\end{aligned} \tag{12}$$

where $\alpha_b = \bar{\alpha}$, the amplitude of α-oscillation data, and $\dot{\alpha}_b$ and $\ddot{\alpha}_b$ represent $ik\,\bar{\alpha}$ and $(ik)^2\,\bar{\alpha}$, respectively. The phase functions PD_j, which represent the phase lag effect, are given by the Padé approximants of order 2:

$$PD_j = \frac{P_{1j}(ik)^2 + P_{2j}(ik)}{P_{3j}(ik)^2 + (ik) + P_{4j}} \tag{13}$$

Equation (12) is the model equation for unsteady aerodynamics to be set up through analysis of a set of forced-oscillation test data obtained with different reduced frequencies k. The data obtained at each k are first Fourier analyzed to result in m Fourier components with frequency jk, where $j = 1, \ldots, m$. Then the same jk Fourier components from the whole set of data are combined to obtain the final model equation in a form similar to Theodorsen's solution in two-dimensional incompressible flow. The coefficients C_j, E_{ij}, H_{ij}, and P_{ij} in the model equation are determined numerically through a least-square analysis. The Padé approximants represent the phase-lag effect, similar to the Theodorsen function. The E_1 and E_2 terms in Eq. (12) represent the zero-lag effect, similar to the virtual mass effect in incompressible flow. Note that in the E terms, the subscript j indicates the Fourier component with frequency jk. Thus, the term with $j = 1$ is associated with the C_1 component, $j = 2$ is associated with the C_2 component (frequency $= 2k$), and so forth.[11] With this modeling technique, the lift response computed with all terms in Eq. (12) is found to be dominated by the first harmonic term (i.e., the C_1 term in Eq. 12), with the higher harmonic terms modifying only the shapes of the C_L curves near both ends (see Figs. 2 and 3). In the present application, it has been verified numerically that the lift coefficient computed with Eq. (12) varies with the amplitude of α oscillation by less than 0.5% at a given frequency for the range of amplitude from 10 to 45 deg (Ref. 12). However, in general, the C_1 term is much larger in magnitude as exhibited by the larger C_L hysteresis than that by the linear theory at the same oscillation amplitude.

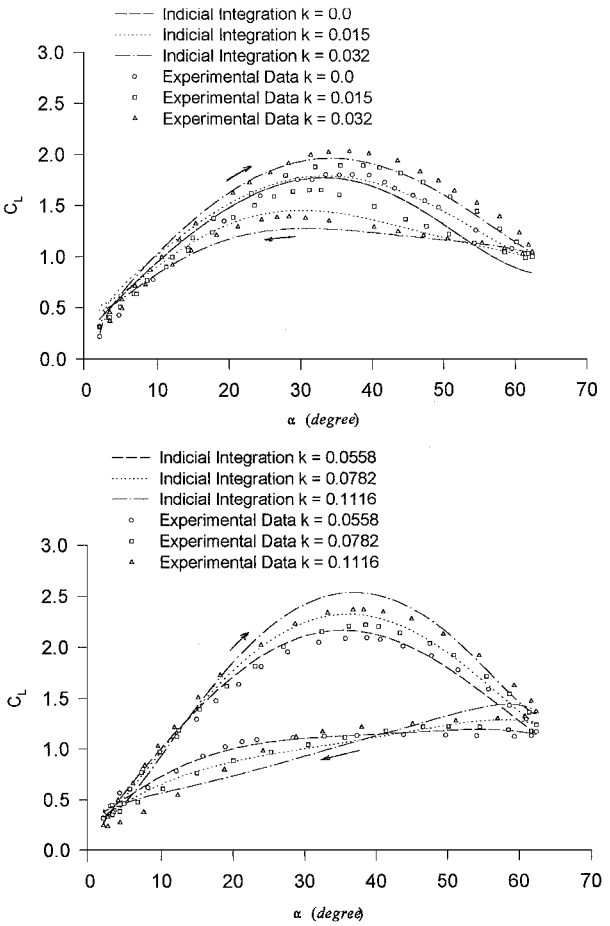

a) Nonlinear model

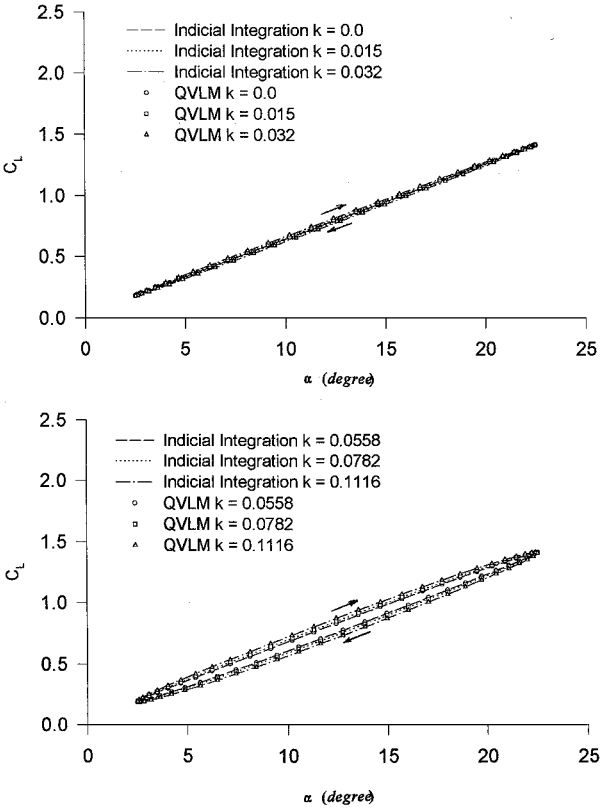

b) Linear model

Fig. 2 C_L responses for nonlinear and linear models of the F-18 HARV configuration.

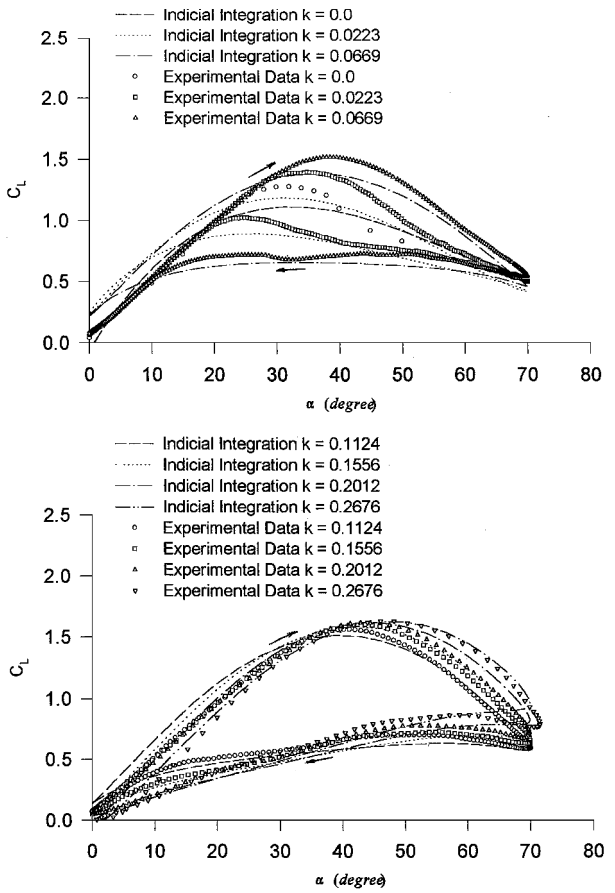

Nonlinear model

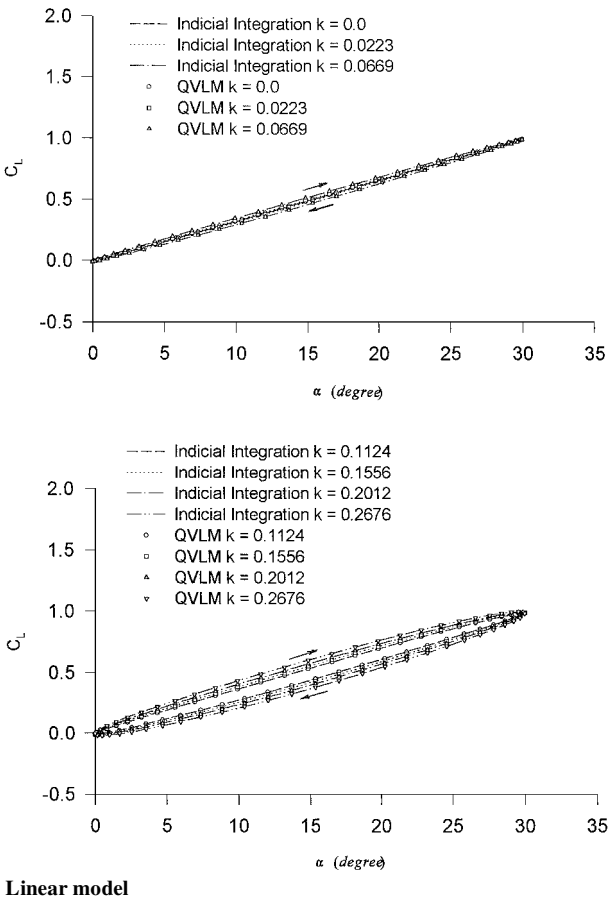

Linear model

Fig. 3 C_L responses for nonlinear and linear models of the F-16XL configuration.

The response function in the time domain can be obtained by using the inverse Fourier transform of Eq. (12) and has the form similar to Eq. (1), that is,

$$h_y(t) = h_y(0) + \text{zero-lag response} + \int_0^t h_{y\alpha}[(t-\tau);\alpha(\tau),\dot{\alpha}(\tau)]\frac{\mathrm{d}\alpha(\tau)}{\mathrm{d}\tau}\,\mathrm{d}\tau + \frac{l}{V}\int_0^t h_{y\dot{\alpha}}[(t-\tau);\alpha(\tau),\dot{\alpha}(\tau)]\frac{\mathrm{d}\dot{\alpha}(\tau)}{\mathrm{d}\tau}\,\mathrm{d}\tau = Kx(-t+t_0) \tag{14}$$

where the α and $\dot{\alpha}$ subscripts of h_y imply partial differentiation with respect to α_b and $\dot{\alpha}_b$.

These integrals have the same forms as those given in Ref. 13 and are obtained through the concept of indicial functions, not the convolution integrals. The equation is used to represent the present unsteady lift model obtained from test data. To perform a numerical time integration, $\alpha(t)$ must be known as a function of time.

The lower part of Fig. 1 shows how the critical gust profile and the maximum airplane aerodynamic lift response are obtained. Based on the MFT method, the time history of impulsive response $h_y(t)$ is reversed in time to obtain the matched excitation waveform as the input to the gust filter. As shown in the lower part of Fig. 1, the excitation wave input to the gust filter still has the same form as that given by Eq. (1) and is denoted as the same $x(t)$. This excitation that produces the maximal response will be defined as the critical gust profile. The critical gust profile in the frequency domain is then obtained as

$$W_g(\omega) = G(\omega)X(\omega) \tag{15}$$

Applying the Fourier transform to Eq. (1), the impulsive response of the combined gust/airplane system can be obtained as

$$H_y(\omega) = KX(-\omega)\,e^{-i\omega t_0} = KX^*(\omega)e^{-i\omega t_0} \tag{16}$$

where the superscript * means complex conjugate. Solving Eq. (16) for X^* and taking the complex conjugate on both sides, Eq. (16) becomes, with $H_y(\omega)$ given by Eq. (11),

$$X(\omega) = (\alpha_0/K)\bar{H}_y^*(\omega)G^*(\omega)e^{-i\omega t_0} \tag{17}$$

Then, substituting Eq. (17) into Eq. (15) and taking the inverse Fourier transform, the critical gust profile in the time domain becomes

$$W_g(t) = \frac{\alpha_0}{2\pi\sigma_y}\int_{-\infty}^{\infty} G(\omega)G^*(\omega)\bar{H}_y^*(\omega)e^{i\omega(t-t_0)}\,\mathrm{d}\omega \tag{18}$$

where $W_g(t)$ is dimensionless. In the present investigation, K is chosen to be σ_y, which can be calculated numerically as, after substituting Eq. (17) into Eq. (5),

$$\sigma_y = \left[\frac{\alpha_0^2}{2\pi}\int_{-\infty}^{\infty} G(\omega)G^*(\omega)\bar{H}_y(\omega)\bar{H}_y^*(\omega)\,\mathrm{d}\omega\right]^{\frac{1}{2}} \tag{19}$$

The critical angle-of-attack profile is then obtained from the critical gust profile:

$$\alpha_g(t) = \tan^{-1}[W_g(t)] \approx W_g(t) \tag{20}$$

After determining the critical gust profile, the time-domain response [Eq. (14) with $\alpha(t)$ replaced by $\alpha_g(t)$] can then be calculated. The time rate of change in the angle of attack $\dot{\alpha}_g$ is obtained by using a central difference method in the present calculation. Note that in wind-tunnel testing, the $\dot{\alpha}$ and q effects on the aerodynamic response cannot be separated. Because in the current study only the $\dot{\alpha}$ effect is incorporated, the q effect in the test data may affect the results somewhat. Later we will present numerical results to identify the magnitude of this q effect for a configuration.

To compare with the nonlinear unsteady aerodynamic effect, a linear unsteady aerodynamic model is calculated with the unsteady quasi-vortex-latticemethod[14] (QVLM), which is similar to the DLM method. The linear aerodynamic models are set up in the same way as the nonlinear one by using the Fourier functional analysis, except that only the first harmonic component is present. For this purpose, the unsteady QVLM code is used to calculate the amplitude of lift response in the frequency domain for given mean angles of attack and oscillation amplitude. For the lift response at a given reduced frequency, the corresponding lift coefficient and angle of attack can be obtained as

$$C_L(t) = \mathrm{Re}\left(\left(C_{L_{\mathrm{Re}}} + iC_{L_{\mathrm{Im}}}\right) * \{\cos(kt) + i[\sin(kt)]\}\right)$$

$$= C_{L_{\mathrm{Re}}} * \cos(kt) - C_{L_{\mathrm{Im}}} * \sin(kt)$$

$$\alpha = \Delta\alpha\cos(kt) \tag{21}$$

By assuming different reduced frequencies, several $C_L \sim \alpha$ curves are generated. These curves are then combined into a linear unsteady aerodynamic model through Fourier functional analysis with only the first harmonic term.

Maximum Gust Response in Vertical Plunging

If the gust response in the presence of airplane's motion is considered, there will be two forcing functions of the same form as Eq. (14), one being C_{L_g} due to the vertical gust velocity component normal to the flight path of airplane and the other being C_{L_m} due to the ensuing motion. The gust is assumed uniform in the spanwise direction. The airplane is assumed to be rigid and only the plunging motion of airplane will be considered. Vertical displacement is defined as positive downward. The plunging-only equation can be used to determine the ride quality and structural loads in a random gust. For airplanes, ride quality in gust is related to the resulting maximum normal acceleration or the maximum incremental load factor.

The plunging equation of motion based on an inertial coordinate system is given by (see p. 299 of Ref. 9)

$$M\ddot{z}(t) = -L_m(t) - L_g(t) \tag{22}$$

To illustrate the formulation, consider a rigid airplane with quasi-steady aerodynamics. Lift generation is instantaneous, that is, there is no time lag in the buildup of lift. Therefore, the plunging-only equation of motion is

$$M\ddot{z}(t) = -\tfrac{1}{2}\rho V^2 S C_{L_\alpha}[\dot{z}(t)/V + W_g(t)] \tag{23}$$

By taking the Fourier transform of Eq. (23) with $W_g(t)$ replaced by a unit impulse function, the aerodynamic transfer function of airplane's vertical displacement due to gust can be expressed as

$$H_y(\omega) = \frac{-\frac{1}{2}\rho V S C_{L_\alpha}}{M(-\omega^2) + \frac{1}{2}\rho V S C_{L_\alpha}(i\omega)} \tag{24}$$

Then the mean square of the vertical displacement of airplane can be obtained as

$$\sigma_z^2 = \int_0^\infty \Phi_{yy}(\omega)\,\mathrm{d}\omega = \int_0^\infty |H_y(\omega)|^2 \Phi_{W_g W_g}(\omega)\,\mathrm{d}\omega \tag{25}$$

where $\Phi_{W_g W_g}(\omega)$ is again given by the approximate von Kármán PSD function. To find the mean square of the normal acceleration, with zero initial conditions,

$$\ddot{z}(t) = \mathscr{F}^{-1}(-\omega^2 \bar{z}) \tag{26}$$

Therefore, the mean square of the normal acceleration is

$$\sigma_{\ddot{z}}^2 = \int_0^\infty \omega^4 |H_y(\omega)|^2 \Phi_{W_g W_g}(\omega)\,\mathrm{d}\omega \tag{27}$$

When unsteady aerodynamic effects are considered, the lift coefficient C_L is now a function of time t. Equation (22) is written as

$$M\ddot{z}(t) = -\tfrac{1}{2}\rho V^2 S C_{L_m}(t) - \tfrac{1}{2}\rho V^2 S C_{L_g}(t) \tag{28}$$

The angle of attack due to motion is approximated by

$$\alpha(t) = \tan^{-1}[\dot{z}(t)/V] \approx [\dot{z}(t)/V] \tag{29}$$

To determine the impulsive response, an impulsive change in gust angle of attack, $\alpha_0\delta(t)$, is imposed. The Fourier transform of $C_{L_g}(t)$ together with the gust model gives

$$\mathscr{F}\left[C_{L_g}(t)\right] = \alpha_0 \bar{C}_{L_g}(\omega) G(\omega) \tag{30}$$

Taking the Fourier transform of Eq. (28) results in

$$\bar{\alpha}(\omega)G(\omega) = \bar{H}_y(\omega)G(\omega)$$

$$= \frac{-(\alpha_0/2)\rho V^2 S \bar{C}_{L_g}(\omega) G(\omega)}{(i\omega)MV + \frac{1}{2}\rho V^2 S\left[\bar{C}_{L_m}(\omega)\big/\,\bar{\alpha}(\omega)\right]} \tag{31}$$

where $\bar{C}_{L_m}(\omega)$ is the lift coefficient obtained in harmonic oscillations in α with an amplitude equal to $\bar{\alpha}(\omega)$. This expression is used in Eq. (18) to determine the critical gust profile. The impulsive response in Eq. (31) contains lift due to motion $[\bar{C}_{L_m}(\omega)]$ and gust $[\bar{C}_{L_g}(\omega)]$. As indicated before, the ratio $\bar{C}_{L_m}(\omega)/\bar{\alpha}(\omega)$ has been shown to be approximately constant.

With the same procedures as in calculating the maximum lift response without the airplane's motion being considered, the critical gust profile in the time domain [Eq. (18)] and the numerical value of the root mean square of the impulsive response of the gust/airplane system can be obtained as shown in Eq. (19).

With the critical gust profile determined, the response in the time domain is to be computed. Equation (22) is rewritten as

$$MV\dot{\alpha}(t) + \tfrac{1}{2}\rho V^2 S C_{L_m}(t) = -L_g(t, \alpha_g, \dot{\alpha}_g) \tag{32}$$

Taking the Fourier transform of Eq. (32), the frequency response of the amplitude function can be obtained as

$$\bar{\alpha}(\omega) = \frac{-L_g(\omega)}{(i\omega)MV + \frac{1}{2}\rho V^2 S\left[\bar{C}_{L_m}(\omega)\big/\,\bar{\alpha}(\omega)\right]} \tag{33}$$

The calculated amplitude function is the change in angle of attack due to the critical gust. From Eqs. (26) and (29), the incremental normal acceleration can be obtained:

$$\ddot{z}(t) = \mathscr{F}^{-1}[(i\omega)V\bar{\alpha}(\omega)] \tag{34}$$

The time history of the incremental load factor can be obtained as

$$\Delta n(t) = -\ddot{z}(t)/g \tag{35}$$

Results and Discussion

Test Data and Aerodynamic Models

In the present investigation, two existing airplane configurations and their dynamic wind-tunnel test data are used to set up the nonlinear unsteady aerodynamic models. The forced harmonic motion test was conducted by sinusoidally oscillating the airplane models at some mean angles of attack and amplitudes. These models include the following:

1) An F-18 High Alpha Research Vehicle (HARV) configuration[15] for which, for the nonlinear unsteady aerodynamic models, the range of angles of attack covered from 2.5 to 62.5 deg with a mean angle of attack of 32.5 deg and amplitude of 30.0 deg. For the linear unsteady aerodynamic models, the angles of attack range from 2.5 to 22.5 deg. Data were measured at reduced frequencies: k =0.0, 0.015, 0.032, 0.0558, 0.0782, and 0.1116.

2) An F-16XL configuration[16] for which, for the nonlinear unsteady aerodynamic models, the model was oscillated about a mean angle of attack of 35.0 deg with an amplitude of 35.0 deg and with the angle of attack ranging from 0.0 to 70.0 deg. With linear unsteady aerodynamics, the model is generated with a mean angle of attack at 15.0 deg and an amplitude of 15.0 deg, that is, with the angles of attack ranging from 0.0 to 30.0 deg. Data were measured at reduced frequencies: k =0.0, 0.0223, 0.0669, 0.1124, 0.1556, 0.2012, and 0.2676.

The nonlinear unsteady aerodynamic model of the F-18 HARV configuration has been analyzed by using five Fourier modes in

Ref. 15. The F-16XL data are analyzed here with three Fourier terms to set up the nonlinear unsteady aerodynamic model. The results of lift coefficient by the indicial integration at the same reduced frequencies are compared with the experimental data for the nonlinear models and with the results from the unsteady QVLM code for the linear models. Figure 2a shows the comparison of nonlinear unsteady lift coefficients of the F-18 HARV configuration, and Fig. 2b shows the same comparison of linear unsteady lift coefficients. Figure 3 presents the same comparison for the F-16XL configuration. Figures 2 and 3 show the experimental lift variation to the change in angle of attack to be much different from the linear theory. Because the F-18 HARV configuration is mostly viscous effect dominated, its nonlinearity at high angles of attack mostly comes from the viscous flow effect, that is, dynamic stall. The aerodynamics of the F-16XL configuration is mainly affected by the vortex-separated flow and the location of vortex bursting. In this case, only three Fourier modes are chosen in the indicial integration for the nonlinear models. As for the linear results in Figs. 2 and 3, the models all show very good agreement with the results from the QVLM code.[14]

A small-amplitude oscillatory model derived from the large-amplitude forced oscillation data was prepared for the F-18 HARV configuration for the purpose of gust response analysis. The analysis sets the mean angle of attack at 12.5 deg and the amplitude of oscillation at 10.0 deg, which covered the range of angle of attack from 2.5 to 22.5 deg. With the same reduced frequencies on which the large-amplitude oscillation model is based, this new set of lift coefficients is generated through indicial integration. These results are presented in Fig. 4.

Before presenting some results of gust response, there are two parameters that need to be specified. First, the scale of turbulence L is set to 2500 ft as specified in FAA-ADS-53 for the purpose of illustration. The value of this scale of turbulence determines the frequency at which the knee of the PSD function curve occurs.[1] Second, the gust velocity or root mean square of gust velocity σ_g is set to 66.0 ft/s for both the F-18 HARV and the F-16XL cases.

Maximum Gust Response in Lift

The F-18 HARV configuration is assumed to be at a Mach number of 0.2. Assume an impulse strength $\alpha_0 = 10.0$ deg ($=0.1745$ rad) for both the nonlinear and linear lift models. The mean aerodynamic chord that is used to nondimensionalize the circular frequency equals 11.52 ft. Based on the established aerodynamic models mentioned earlier, the first step as depicted in Fig. 1 is to determine the critical gust profile [Eq. (18)]. In performing the inverse Fourier transform in Eq. (18), the integration limits are theoretically from negative infinity to positive infinity. Practically, the frequency range is finite in the numerical integration. Because the experimental data were obtained for a limited range of reduced frequency, a proper selection of the frequency range is assumed to be one that will result in the maximum lift response consistent with the original experimental data. In all results to be presented, t_0 is assumed zero. Through numerical experimentation, it is determined that $|k| \leq 1.5$ for the F-18 HARV and $|k| \leq 2.2$ for the F16XL. Figure 5 shows gust responses with nonlinear and linear aerodynamics for the F-18 HARV. Figure 5 contains three plots: the upper two plots are the critical angle of attack profiles [Eq. (20)], and the corresponding time rates of change in angle-of-attack; the bottom plot is the corresponding lift response. The upper two plots show that the resulting angle-of-attack profiles and time rates of change are practically the same for the nonlinear and linear aerodynamic models. However, the lift response is higher if nonlinear aerodynamics is used. It shows that the maximum lift coefficient with nonlinear unsteady aerodynamics is 2.079. This is higher than the linear unsteady aerodynamic model with a maximum lift coefficient equal to 1.376 by 51.1%. The main reason for this large difference is because of the $\dot{\alpha}$ (or frequency) effect in that the first harmonic response [the C_1 term in Eq. (12)] is much higher in nonlinear aerodynamics than in linear aerodynamics.

Note that, in the present application of MFT, the impulse strength α_0 is equivalent to the impulse strength K used by Pototzky et al.[5] In Ref. 7, the impulse strength K was varied from 10 to 15,000 to perform a one-dimensional search for the critical gust profile in a system with nonlinear controllers. In the present investigation,

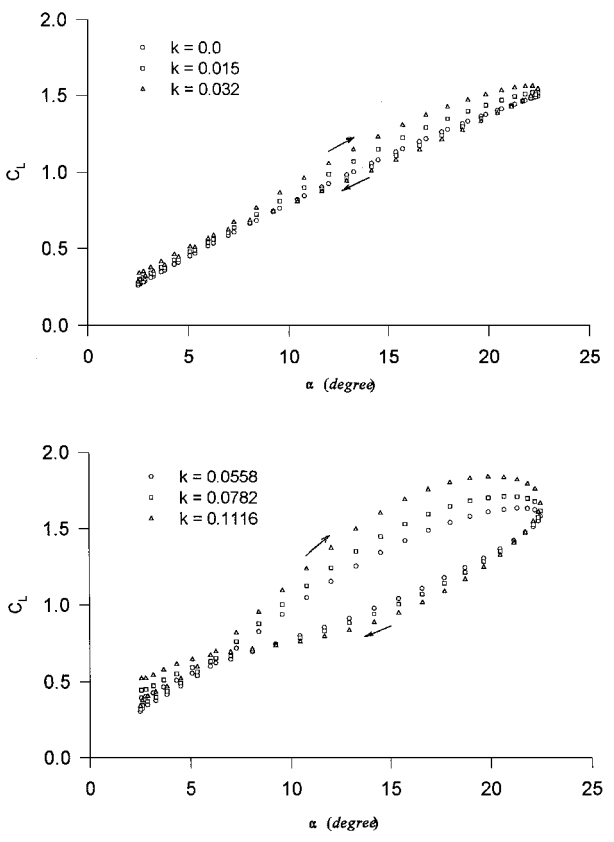

Fig. 4 Derived small-amplitude aerodynamic models for the F18 HARV configuration.

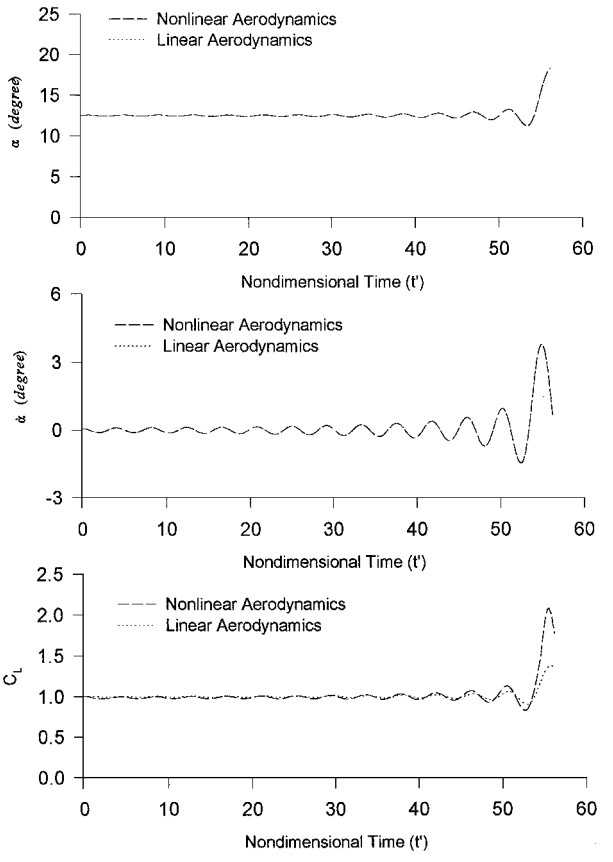

Fig. 5 Critical gust profile and maximal C_L response for the F-18 HARV configuration.

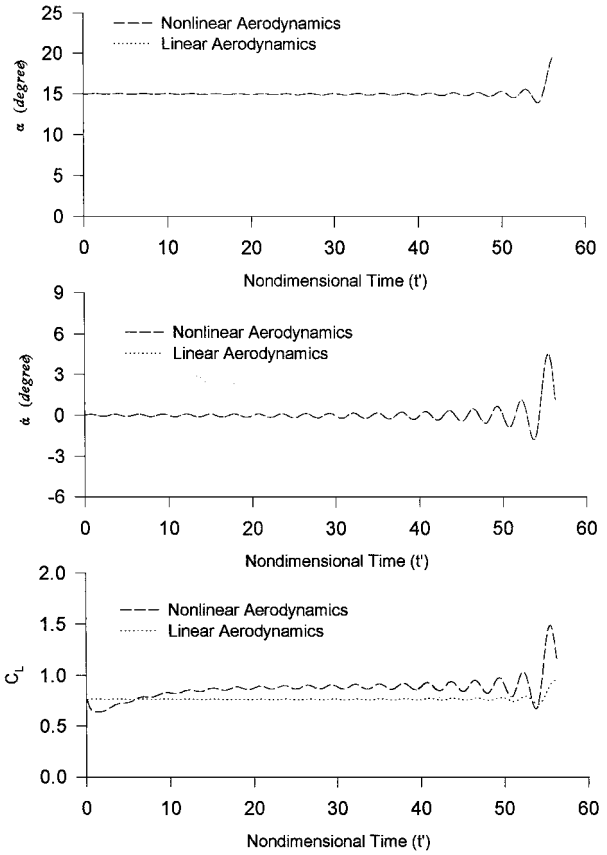

Fig. 6 Critical gust profile and maximal C_L response for the F-16XL configuration.

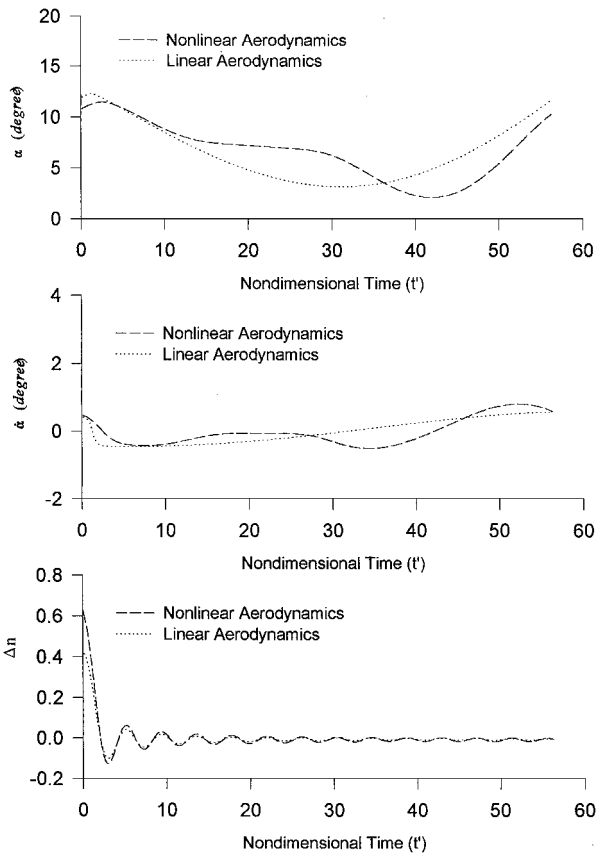

Fig. 7 Critical gust profile and maximal load factor for the F-18 HARV configuration in plunging motion.

the impulse strength is assumed to be $\alpha_0 = 10.0$ deg for the F-18 HARV configuration. The increase of α_0 does cause the critical gust profile and the subsequent gust response to change slightly. For example, increasing α_0 from 10.0 to 15.0 deg for the same F-18 HARV configuration with the other factors being fixed, the maximum lift coefficient is calculated to increase by the order of 10^{-6}. Therefore, the effect of limited variation of impulse strength in the present study is minor. This conclusion is also true for the F-16XL configuration.

The flight condition for the F-16XL configuration is again assumed to be at a Mach number of 0.2. The impulse strength is taken to be $\alpha_0 = 35.0$ deg ($=0.6109$ rad) for the nonlinear aerodynamic model because test data obtained at an oscillation amplitude of 35 deg are available and $\alpha_0 = 15.0$ deg ($=0.2618$ rad) for the linear aerodynamic model. The mean aerodynamic chord that is used to nondimensionalize the circular frequency equals 24.7 ft. Figure 6 shows the lift response to gust with nonlinear and linear aerodynamics. Figure 6 contains the same three plots as shown in Fig. 5. Again, Fig. 6 shows that the resulting critical angle of attack and the time rates of change profiles are indistinguishable between the nonlinear and linear aerodynamics. In Fig. 6, the maximum lift coefficient is 1.491 for the nonlinear aerodynamic model and is higher than the lift coefficient of 0.951 for the linear aerodynamic model by 56.8%.

Maximum Gust Response in Vertical Plunging

The purpose of incorporating airplane's plunging equation of motion in the present gust response analysis is to determine the maximum incremental load factors with linear or nonlinear unsteady aerodynamics. The airplane is assumed rigid.

The weight of F-18 HARV is assumed to be 30564.7 lbf, and the wing reference area is 400.0 ft^2. The large-amplitude nonlinear and linear unsteady aerodynamic models are used to calculate the critical gust profiles with an impulse strength $\alpha_0 = 30.0$ deg. The root mean square gust velocity is again assumed to be $\sigma_g = 66.0$ ft/s. The freestream velocity V is 223.2 ft/s, which results in a dynamic pressure $q = 59.2$ lbf/ft^2.

The critical gust profile is obtained from Eq. (18) with $\bar{H}_y(\omega)G(\omega)$ defined by Eq. (31).

Comparison of the critical angle of attack and the corresponding time rates of change in angle of attack with either linear or nonlinear unsteady aerodynamics are shown in the upper two plots of Fig. 7 for the F-18 HARV. These two plots show that the critical gust profiles are no longer identical for the linear and nonlinear unsteady aerodynamics. The bottom plot is the resulting time history of the incremental load factor. Because the z axis is defined as positive downward, the resulting negative gust load factor means that the airplane is responding to an upward gust. For nonlinear unsteady aerodynamics, the maximum upward incremental load factor is equal to 0.620 and the maximum downward load factor is 0.127. If the linear unsteady aerodynamics are considered, the maximum upward incremental load factor is 0.417 and the maximum downward load factor is 0.101. The numerical results show the maximum upward incremental load factor occurred at the initial time because t_0 is assumed zero. The airplane will experience a downwash as it moves upward. The current numerical results also show that the maximum upward incremental load factor for nonlinear unsteady aerodynamics is higher than that for linear unsteady aerodynamics by 48.7%. This result indicates that the F-18 HARV airplane with a moderately swept wing is sensitive to the effect of nonlinear unsteady aerodynamics. Again, the large difference in the incremental load factors comes from the $\dot{\alpha}$ effect.

For the F-16XL, the weight is taken to be 43,000.0 lbf, and the wing reference area is 600.0 ft^2. The same large-amplitude ($\alpha_0 = 35.0$ deg) nonlinear and small-amplitude ($\alpha_0 = 15.0$ deg) linear unsteady aerodynamic models as used earlier are used to calculate the critical gust profiles and their corresponding responses. In addition, $\sigma_g = 66.0$ ft/s and $V = 223.2$ ft/s, which results in a dynamic pressure $q = 59.2$ lbf/ft^2.

The critical angle of attack and rate of change in angle-of-attack profiles are shown in the upper two plots of Fig. 8. It shows that the critical gust profiles are again different with the linear and nonlinear unsteady aerodynamics. The bottom plot shows that the maximum upward incremental load factor is equal to 0.521 and the maximum

Table 1 Calculated Δn_{max} from different aerodynamic models

Model	Quasi-steady	Linear unsteady	Nonlinear unsteady
F-18 HARV	0.267	0.417	0.620
F-16XL	0.318	0.274	0.521

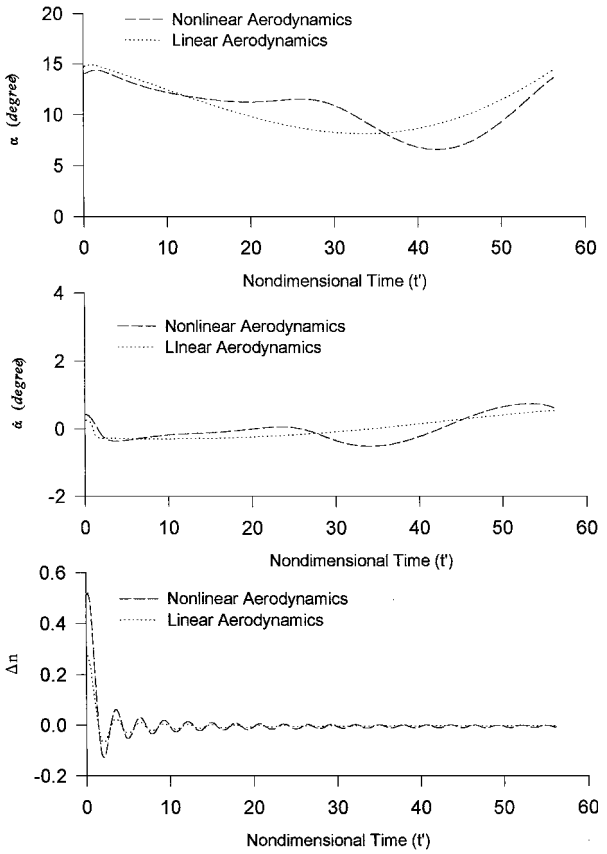

Fig. 8 Critical gust profile and maximal load factor for the F-16XL configuration in plunging motion.

downward load factor is 0.127 for the nonlinear unsteady aerodynamics. With the linear unsteady aerodynamics, the maximum upward incremental load factor is 0.274 and the maximum downward load factor is 0.070. Therefore, the maximum load factor with a nonlinear unsteady aerodynamic model is 90.1% higher than that with linear unsteady aerodynamics.

Analysis based on quasi-steady aerodynamics [Eq. (23)] has also been performed. The lift curve slopes C_{L_α} in Eq. (23) are obtained from static lift curves and are found to be 5.797 and 2.530/rad for the F-18 HARV and F16XL, respectively. The results for Δn_{max} are compared with other aerodynamic models in Table 1. It is seen that quasi-steady approximation is inadequate in predicting Δn_{max} for the F-18 configuration with a moderate aspect ratio.

Theoretically, plunging, rather than pitching, oscillation data should have been used in Eqs. (31) and (32). To see the difference, Δn_{max} for the F-18 HARV based on linear plunging aerodynamics is calculated, and is equal to 0.387, as compared with 0.417 with the pitching model. This result shows that the q effect in the linear aerodynamic model increases the predicted Δn_{max} in plunging motion by 7.7%.

Conclusion

A method to incorporate nonlinear unsteady aerodynamics in the MFT in determining gust response was developed. These nonlinear unsteady aerodynamics were obtained through analysis of experimental data by forced oscillation testing. This new process of analysis showed that using the more realistic nonlinear unsteady aerodynamic models would produce at least 50–60% higher maximum lift response than the linear theory for the F-18 HARV and the F-16XL under the prescribed von Kármán gust. With the airplane in the plunging-only motion, the nonlinear unsteady aerodynamics produced 48.7–90.1% higher maximum incremental load factors to the von Kármán gust than the linear unsteady aerodynamics for the F-18 HARV and the F-16XL. The main reason for the large difference was the effect of the time rate of change in angle of attack.

Acknowledgment

This research was partially supported by the Kansas Center for Advanced Scientific Computing at the University of Kansas.

References

[1]Hoblit, F. M., *Gust Loads on Aircraft: Concepts and Applications*, AIAA Education Series, AIAA, Washington, DC, 1988, pp. 29–46.

[2]Federal Aviation Regulations, Part 25: Airworthiness Standards: Transport Category Airplanes, Change 15, Eff. 10/14/80, Federal Aviation Administration, U.S. Dept. of Transportation, Washington, DC, 1980.

[3]Perry, B., III, Pototzky, A. S., and Woods, J. A., "NASA Investigation of a Claimed Overlap Between Two Gust Response Analysis Method," *Journal of Aircraft*, Vol. 27, No. 7, 1990, pp. 605–611.

[4]Pototzky, A. S., Zeiler, T. A., and Perry, B., III, "Calculating Time-Correlated Gust Loads Using Matched Filter and Random Process Theories," *Journal of Aircraft*, Vol. 28, No. 5, 1991, pp. 346–352.

[5]Scott, R. C., Pototzky, A. S., and Perry, B., III, "Maximized Gust Loads for a Nonlinear Airplane Using Matched Filter Theory and Constrained Optimization," NASA TM 104138, 1991.

[6]Scott, R. C., Pototzky, A. S., and Perry, B., III, "A Computer Program to Obtain Time-Correlated Gust Loads for Nonlinear Aircraft Using the Matched-Filter Based Method," Federal Aviation Administration, DOT/FAA/CT-93/63, U.S. Dept. of Transportation, Washington, DC, Feb. 1994.

[7]Scott, R. C., Pototzky, A. S., and Perry, B., III, "Computation of Maximized Gust Loads for Nonlinear Aircraft Using Matched-Filter-Based Schemes," *Journal of Aircraft*, Vol. 30, No. 5, 1993, pp. 763–768.

[8]Haykin, S., *Communication Systems*, Wiley, New York, 1978, pp. 594–596.

[9]Fung, Y. C., *An Introduction to the Theory of Aeroelasticity*, Dover, New York, 1969, pp. 275–280.

[10]Barr, N. M., Gangaas, D., and Schaeffer, D. R., "Wind Tunnel Models for Flight Simulator Certification of Landing and Approach Guidance and Control Systems," Final Rept., FAA-RD-74-206, Boeing Commercial Airplane Co., Seattle, WA, 1974.

[11]Chin, S., and Lan, C. E., "Fourier Functional Analysis for Unsteady Aerodynamic Modeling," *AIAA Journal*, Vol. 30, No. 9, 1992, pp. 2259–2266.

[12]Lee, Y. N., "Nonlinear Analysis of Random Gust Response," Ph.D. Dissertation, Dept. of Aerospace Engineering, Univ. of Kansas, Lawrence, KS, Dec. 1998.

[13]Tobak, M., and Schiff, L. B., "On the Formulation of the Aerodynamic Characteristics in Aircraft Dynamics," NASA TR R-456, Jan. 1976.

[14]Lan, C. E., "Unsteady Suction Analogy and Applications," *AIAA Journal*, Vol. 20, No. 12, 1982, pp. 1647–1656.

[15]Hu, C. C., Lan, C. E., and Brandon, J. M., "Unsteady Aerodynamic Models for Maneuvering Aircraft," AIAA Paper 93-3626, Aug. 1993.

[16]Wang, Z. J., Lan, C. E., and Brandon, J. M., "Fuzzy Logic Modeling of Nonlinear Unsteady Aerodynamics," AIAA Paper 98-4351, Aug. 1998.

A. Plotkin
Associate Editor